Romanian Reports in Physics **72**, 804 (2020)

A MONTE CARLO STUDY ON THE DOSE DISTRIBUTION IN THE VOLUME OF THE GLASS SAMPLES USED IN DOSIMETRY APPLICATIONS

M. ZADEHRAFI[1,2], C. OLARU[1], G. ORMENISAN[1], S. CIOBANU[1]

[1] "Horia Hulubei" National Institute for Physics and Nuclear Engineering,
30 Reactorului, P.O.Box MG-6, RO-077125 Bucharest-Magurele, Romania
[2] University of Mazandaran, Department of Physics, Faculty of Basic Science,
P.O.Box 47415-416, Balbosar, Iran
E-mail: *mastaneh.zadehrafi@nipne.ro*

Received February 28, 2020

Abstract. In this paper, a Monte Carlo study on the dose distribution in the volume of the glass samples used in dosimetry applications was performed. Due to the fact that in glass-based dosimetry the calibration process plays a very important role, it must be carefully approached. In this mater, a study on the influence of the energy of the involved ionizing radiation as well as the position (rotational plan) of the glass samples to the resulting dose distribution was done. Three arbitrary photon energy values, namely 100 keV, 150 keV, and 200 keV, and two angular positions (0 and 45 degrees angle) were chosen. It was shown that when "reading" the optical parameters of the exposed glass samples, due to the sensitivity of the dose distribution to energy and position, it is very important to be done on the best possible aligned samples. It is also recommended to make multiple determinations on the same sample and use the mean value. By using a mean value, more precise and more accurate values can be obtained, as well as a better evaluation of the associated budget of uncertainties.

Key words: Monte Carlo, dose distribution, glass-based dosimetry.

1. INTRODUCTION

Due to their specific optical proprieties and also their low cost, glass-based optical materials are widely used in many applications. In this paper, the main focus is on their usage in the nuclear physics field. Here, the glass is used on multiple applications, including dosimetry [1–5], which is the science of measuring the dose and the associated quantities. The dosimetry may be approached in different ways, meaning in applications that do not necessarily involve precise measurements, but also in the metrology of dose. The latest involves a more careful approach and also some metrology – specific aspects as traceability, precision, accuracy, uncertainty estimation, etc. In order to fulfill all these requirements, every involved aspect must be carefully addressed. In this paper, the main focus is on the calibration part of the glass-based dosimetry.

The glass-based dosimetry is a part of the dosimetry that applies glass samples as detectors and a "reading" procedure for the associated parameters that are proportional to the absorbed dose. These parameters will change when the samples are exposed to specific absorbed dose values (due to the energy deposited by the ionizing radiation into the glass volume, leading to the occurrence of the color centers) and the dependence law can be determined by an experimental manner [6–15]. After knowing the dependence law (namely the calibration of the parameter-to-dose response), the glass detectors may be used for determining any unknown dose value.

The part of the calibration process that is the direct subject of this study is the one related to the importance of having as best as possible aligned glass samples, due to the sensitivity of the dose distribution to the incident angle and the energy transported by the ionizing radiation [16]. In this matter, three arbitrary photon energy values, namely 100 keV, 150 keV, and 200 keV, and two angular positions (0 and 45 degrees angles) were chosen. For all the above-mentioned cases, the dose distribution was determined by computational Monte Carlo means.

Monte Carlo is a powerful modeling tool, which can be used to simulate statistical processes such as the interaction of nuclear particles with matter. This method estimates the solution of mathematical problems by generating numerous random numbers. It is particularly competent for complex problems that are hard (or impossible) to be modeled by using deterministic methods. Monte Carlo is a realistic technique, which – in the case of particle transport – actually follows each of many generated particles from the source to the end of its path [17–20]. In this paper, the Monte Carlo MCNP code was used.

MCNP is a general-purpose Monte Carlo N-Particle transport code, which is developed and maintained by Los Alamos National Laboratory [21]. This code deals with several transport modes: neutron only, photon only, electron only, combined neutron/photon transport where the photons are produced by neutron interactions, neutron/photon/electron, photon/electron, or electron/photon. The energy regime is from 10^{-11} MeV to 20 MeV for neutrons, and from 1 keV to 1000 MeV for photons and electrons.

Some important standard features that make MCNP adaptable and easy to use are as follows: Capability to define a wide variety of general, surface, and criticality sources; the ability to plot both geometry and output tally; having an extensive collection of variance-reduction techniques, tally types, and cross-section data.

The geometrical cells in MCNP are bounded by first- and second-degree surfaces and fourth-degree elliptical tori, and can be made from arbitrary materials.

Continuous-energy nuclear and atomic data libraries are included in MCNP. For neutrons, the code takes into account all the reactions given in a particular cross-section evaluation (*e.g.,* ENDF/B-VI). For photons, incoherent and coherent scattering, fluorescent emission after photo-electric absorption, pair production with local emission of annihilation radiation and bremsstrahlung are considered. For electron transport, the code uses a continuous slowing down model that includes positrons, K X-rays, and bremsstrahlung. MCNP uses nuclear data for neutrons and atomic data for photons and electrons.

The version 4C of the code (MCNP-4C) has been used in this work, which is applicable in both Unix and Windows operating systems [22, 23].

2. METHODOLOGY

In this study, a cylindrical BK-7 glass sample with 10 mm height and 25 mm diameter has been modeled by MCNP-4C Monte Carlo code. A gamma-ray point-like source was positioned at 100 cm distance from the center of the mass of the sample. The modeling has been performed for two different positions of the sample relative to the source. At first, the glass sample was facing toward the point source and the source was exactly aligned with the cylindrical axis of the sample. For the second considered case, the sample was rotated with 45 degrees.

Three arbitrary gamma-ray energy values, namely 100 keV, 150 keV, and 200 keV were chosen. The chemical composition of the BK-7 glass sample used in the model is as follows: O (53.5%), Si (37.7%), Na (4.1%), B (3.7%), and Al (1.0 %).

3. RESULTS AND DISCUSSIONS

In both cases (straight and rotated samples), the dose distribution into the glass sample volume (dose as a function of depth and also as a function of the distance from the center of the surface) has been calculated. To investigate the depth dose distribution, the cylindrical sample was divided into 10 disk-shaped samples with the same diameter (25 mm) and 1 mm thickness (Figs. 1a and 1b).

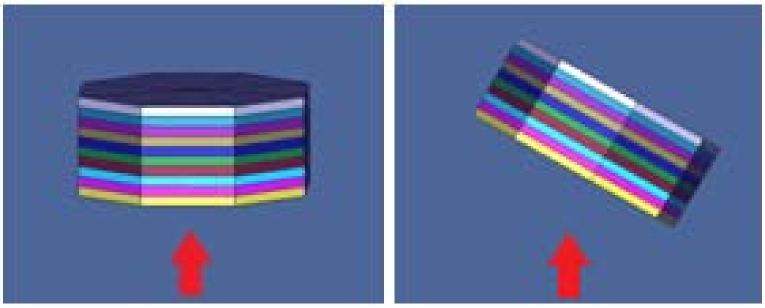

(a) (b)

Fig. 1 – The BK-7 cylindrical sample divided into 10 disk-shaped samples to investigate the depth dose distribution into the glass volume (a) straight position, (b) rotated with 45°.

To investigate the radial dose distribution, two cylinders with 10 mm height and 4 mm radius were considered at each end of the main glass sample (Fig. 2).

These cylinders are indicated with numbers 1 and 2. When the glass sample is rotated, the distance between cylinder 2 and the source is more than of cylinder 1.

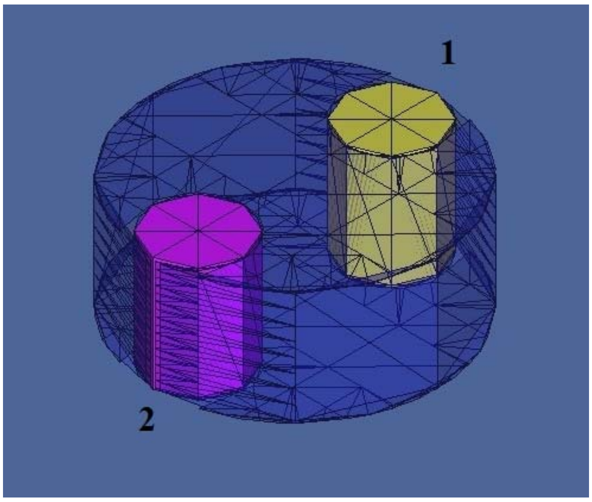

Fig. 2 – Two smaller cylinders inside and at each end of the main glass sample.

Using *f8 tally in MCNP-4C, the energy deposited in the small samples (disks and cylinders) were calculated and by dividing the energy to the mass of each sample, the absorbed doses were obtained. The number of tracked photons (events) was considered as 10^8 in each simulation process. The relative errors were less than 0.01%, in all the calculations.

The absorbed doses as a function of depth inside the BK-7 glass sample (straight positioned), for 100 keV, 150 keV, and 200 keV gamma rays are presented in Fig. 3. As it can be seen, for all three chosen energy values, the absorbed dose value as a function of the depth is first increasing to a maximum value corresponding to 0.15 cm, then starting to slowly decrease. For the chosen energy range, the higher energy led to the higher dose value.

For the case of the 45° rotated sample, the absorbed dose as a function of depth inside the BK-7 glass sample is presented in Fig. 4 (100 keV gamma rays). As it can be observed, in this case, the shape of the graph is way different from the case of the straight positioned sample. The absorbed dose value as a function of the depth is increasing with a higher rate to a maximum value corresponding to 0.65 cm, then starting to decrease (also with a higher rate). As it can be also seen, the magnitude of the overall dose value for rotated sample is two order lower than for the straight case, mostly due to the narrowed source-sample solid angle.

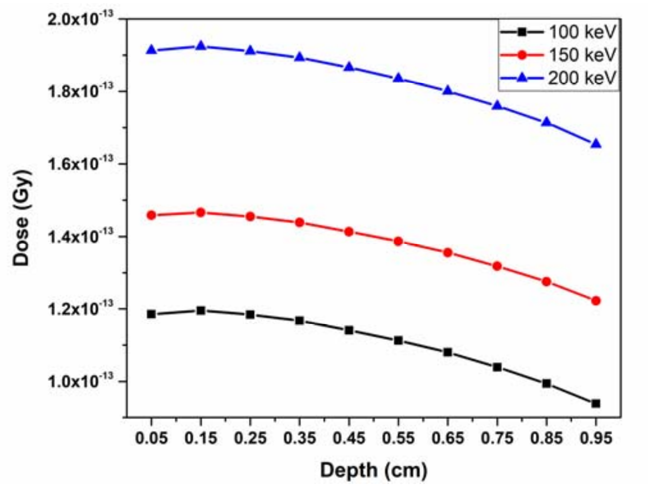

Fig. 3 – The absorbed dose value as a function of depth inside the BK-7 glass sample (straight positioned) for three different gamma-ray energies (100 keV, 150 keV, and 200 keV).

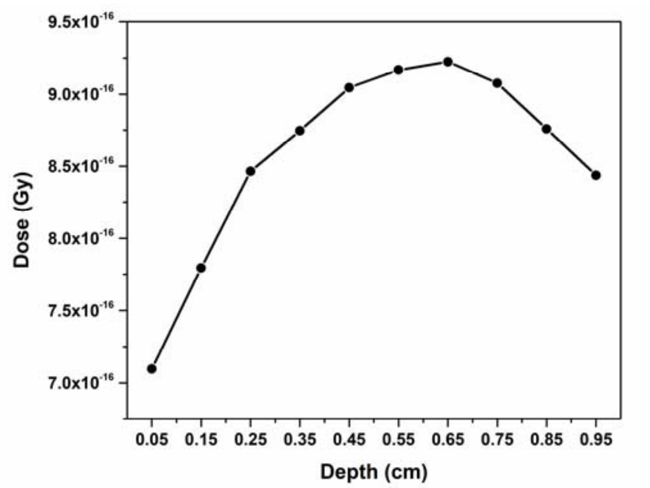

Fig. 4 – Dose value as a function of depth inside the BK-7 glass sample for a 45° rotated sample. The point source is of 100 keV energy.

The results regarding the radial dose distribution, for both straight and rotated samples, are presented in Table 1. When comparing the straight *vs.* rotated cases (for the same energy), a high difference between the absorbed dose value in the cylinder 1 *vs.* cylinder 2 is observed, showing how sensitive is the radial dose distribution to rotational angle of the sample (almost an order of magnitude).

Table 1

Radial dose distribution in the BK-7 glass sample

Sample's position – Energy of the source	**Total absorbed dose in cylinder 1 (×10^{-14}) [Gy]**	**Total absorbed dose in cylinder 2 (×10^{-14}) [Gy]**
Straight – 100 keV	1.34	1.34
Straight – 150 keV	1.26	1.26
Straight – 200 keV	1.36	1.36
45^0 rotated – 100 keV	8.9	0.241

4. CONCLUSIONS

A Monte Carlo study on the dose distribution in the volume of the glass samples used in dosimetry applications was performed. In this mater, a study on the influence of the energy of the involved ionizing radiation as well as the position (rotational plan) of the glass samples to the resulting dose distribution was done. Three arbitrary photon energy values, namely 100 keV, 150 keV and 200 keV, and two rotational positions (0 and 45^o angles) were chosen. It was shown that the dose distribution as a function of depth inside the sample, as well as the radial dose distribution, strongly depend on the sample's rotational position. Due to the sensitivity of the dose distribution to the energy and position, it is very important that the controlled technical irradiation of the glass samples (calibration purposes) to be done on the best possible aligned samples. When analyzing the exposed glass samples, it is recommended to make multiple determinations on the same sample and consider using the mean values. By using a mean value of the analyzed parameters, more precise and more accurate absorbed dose values can be obtained, as well as a better evaluation of the associated budget of uncertainties.

Acknowledgments. This work is supported by the Romanian Ministry of Education and Research through "Proiect Nucleu" PN 19 06 02 04 / 2019.

REFERENCES

1. M. Discher, C. Woda and I. Fiedler, *Improvement of dose determination using glass display of mobile phones for accident dosimetry*, Radiat. Measurements. **56**, 240–243 (2013).
2. S. Yasmin et al., *Thermoluminescence features of commercial glass and retrospective accident dosimetry*, Rad. Phys. Chem. **168**, 108528 (2020).
3. N. binti Wahib et al., *Commercial kitchenware glass as a potential thermoluminescent media for retrospective dosimetry*, Appl. Radiat. Isotopes **148**, 218–224 (2019).
4. J. M. Schwantes et al., *Intrinsic dosimetry of glass containers used to transport nuclear materials: Potential implications to the fields of waste management and nuclear forensics*, Radiat. Measurements **44**, 405–408 (2009).
5. P. Aramrun, N. A. Beresford and M. D. Wood, *Selecting passive dosimetry technologies for measuring the external dose of terrestrial wildlife*, J. Environ. Radioact. **182**, 128–137 (2018).
6. A. Duragkar et al., *Versatility of thermoluminescence materials and radiation dosimetry – A review*, Luminescence **34**, 656–665 (2019).

7. M.-R. Ioan et al., *Laser beam used to measure and highlight the transparency changes in gamma irradiated borosilicate glass*, J. Optoelectron. Adv. M **16**, 162–169 (2014).
8. M.-R. Ioan et al., *3 MeV protons to simulate the effects caused by neutrons in optical materials with low metal impurities*, J. Optoelectron. Adv. M **15**, 523–529 (2013).
9. M.-R. Ioan, *LIDT test coupled with gamma radiation degraded optics*, Opt. Commun. **369**, 94–99 (2016).
10. S.V. Firstov et al., *Radiation-induced absorption in bismuth-doped germanosilicate fibres*, Quantum Electron. **47**, 1120 (2017).
11. M.-R. Ioan, *Investigation of RGB spectral components in the images captured through gamma rays affected optical focusing lens*, Rom. J. Phys. **61**, 1198–1206 (2016).
12. M.-R. Ioan, *Study of the optical materials degradation caused by gamma radiation and the recovery process by controlled heat treatment*, Rom. J. Phys. **61**, 892–902 (2016).
13. Z. Zheng et al., *Window glass as a routine dosimeter for radiation processing*, Int. J Radiat. Appl. Instrum. C Radiat. Phys. Chem. **31**, 419–423 (2002).
14. P. Oonsiri et al., *Investigation of the dosimetric characteristics of radiophotoluminescent glass dosimeter for high-energy photon beams*, J. Radiat. Res. Appl. Sc. **12**, 65–71 (2019).
15. T. Kurobori, *Performance characterisation of a real-time fiber dosimetry system using radiophotoluminescent glasses*, Jpn. J. Appl. Phys. **57**, 106402 (2018).
16. E. Garcia-Torano et al., *A novel radionuclide-specific detector system for the measurement of radioactivity at steelworks*, J. Radioanal. Nucl. Ch. **303**, 293–298 (2015).
17. M. Zadehrafi et al., *"MetroMC" research group: Computational physics in ionizing radiation metrology*, Rom. J. Phys. **65**, 808 (2020).
18. C. Mihai, *Monte Carlo Evaluation of The Energy Deposited by Leptons in The Kascade Grande Detectors*, Rom. J. Phys. **50**, 663–668 (2005).
19. M. Pimpinella et al., *Monte Carlo Calculation of Correction Factors for Dosimetry in Radiotherapy Using The Correlated Sampling Method*, Rom. Rep. Phys. **66**, 109–119 (2014).
20. D. Mihailescu and C. Borcia, *Electron Dose Distributions in Inhomogeneous Phantoms: A Monte Carlo Study*, Rom. Rep. Phys. **70**, 603 (2018).
21. https://mcnp.lanl.gov
22. J. F. Briesmeister (Ed.), MCNP^{TM}, LA-13709-M, V4C (2000).
23. J. K. Shultis and R. E. Faw, *An MCNP primer.* Technical report, Dept. of Mechanical and Nuclear Engineering, Kansas State University, 2011.